



Electrochemical Characterization of Mixed Conducting Ba(Ce_{0.8-y}Pr_yGd_{0.2})O_{2.9} Cathodes

R. Mukundan,^{*,a,z} P. K. Davies, and W. L. Worrell^{**}

Department of Materials Science and Engineering, University of Pennsylvania, Philadelphia, Pennsylvania 19104-6272, USA

The high proton conductivities of doped barium and strontium cerates has led to their consideration as electrolytes in fuel cells operating at intermediate temperatures (600-800°C). The electrochemical properties of Pr-doped barium gadolinium cerate [Ba(Ce_{0.8-y}Pr_yGd_{0.2})O_{2.9}] have been investigated as part of our assessment of new mixed-conducting electrodes in fuel cells with barium cerate electrolytes. Substitution of Pr for Ce increases the total and electronic conductivities, and the total conductivity of Ba(Pr_{0.8}Gd_{0.2})O_{2.9} exceeds ~0.75 S/cm at 800°C in dry air. Electromotive force measurements indicate that the Pr-substituted samples also retain high proton and oxygen-ion conductivities despite their decreased ionic transport numbers. Cathodes prepared using these mixed-conducting Pr-doped barium-gadolinium cerates exhibit low cathodic overpotentials in Ba(Ce_{0.8}Gd_{0.2})O_{2.9} electrolyte fuel cells. For example, the cathodic overpotential resistance of a Ba(Pr_{0.8}Gd_{0.2})O_{2.9} cathode is 0.47 Ω cm² at 800°C at current densities <100 mA/cm². This is the lowest cathodic overpotential resistance reported for a perovskite electrode on a proton-conducting electrolyte fuel cell at this temperature.

© 2000 The Electrochemical Society. S0013-4651(00)08-027-7. All rights reserved.

Manuscript submitted August 7, 2000; revised manuscript received October 11, 2000.

The Sr(Ce_{1-x}M_x)O_{3-x/2}-based perovskites are the first group of proton conductors that can tolerate the temperatures and thermal cycling encountered in solid oxide fuel cell applications.¹ Several studies of cerate-based systems have been reported, and the gadolinium-substituted barium cerates have been found to have some of the highest conductivities in the 700-1000°C range.^{2,3} For example, the proton conductivity (4×10^{-2} S/cm) of Ba(Ce_{0.8}Gd_{0.2})O_{2.9} at 600°C under fuel cell conditions² is comparable to the oxygen-ion conductivity of yttria-stabilized zirconia at 800°C. Thus Ba(Ce_{1-x}Gd_x)O_{3-x/2} ($x = 0.1 - 0.2$) electrolytes have received considerable attention for fuel cell applications.^{2,4} One of the best reported perovskite electrolyte fuel cells² [a Ba(Ce_{0.8}Gd_{0.2})O_{2.9} electrolyte with platinum electrodes] exhibited a short circuit current density of 800 mA/cm² at 800°C.

There is considerable interest in reducing costs and improving cell performances by developing new mixed-conducting oxides to replace the platinum electrodes. Several manganese-based perovskites have been studied as cathodes in Ba(Ce_{1-x}Nd_x)O_{3-x/2} electrolyte fuel cells, and La_{0.6}Ba_{0.4}MnO₃ was found to have the lowest polarization resistance (~1.1 Ω cm² at 800°C).⁵ However, the polarization resistance of this purely electronic conducting cathode is significantly higher than that of platinum (~0.35 Ω cm² at 800°C).⁵

Our studies have focused on new mixed-conducting perovskites that are chemically compatible with the barium cerate-based electrolytes. We have chemically modified barium cerate to produce oxides with a high electronic and ionic (proton and oxygen-ion) conductivity. We have reported the effect of Pr substitution on the electronic and ionic conductivity of 10 mol % Gd-doped barium cerate.^{6,7} The introduction of Pr in the Ba(Ce_{0.9-y}Pr_yGd_{0.1})O_{2.95} solid solutions increases the p-type electronic conductivity and decreases the ionic conductivity.⁶ Preliminary studies also indicated that the cathodic overpotential resistance in Ba(Ce_{0.8}Gd_{0.2})O_{2.9} electrolyte fuel cells can be lowered by using Pr-based mixed conducting cathodes.⁷

The effect of Pr doping in Ba(Ce_{1-x}Gd_x)O_{3-x/2} oxides has also been reported recently.^{8,9} Although an increase in the hole conductivity under oxidizing conditions was observed, the authors wanted to enhance the proton conductivity of these perovskites, so most of their measurements were conducted in H₂ atmospheres. They concluded that the Ba(Pr_xGd_{1-x})O_{3-x/2} ($0.1 < x < 0.4$) oxides were useful electrolytes in fuel cells at temperatures <600°C, and the use of these perovskites as cathodes at elevated temperatures (600-800°C) was not examined. This paper reports our results on the conductivity,

transference number, and cathode performance of the Ba(Ce_{0.8-y}Pr_yGd_{0.2})O_{2.9-y/2} perovskites.

Experimental

Single-phase perovskite samples of Ba(Ce_{0.8-y}Pr_yGd_{0.2})O_{2.9} ($y = 0.4, 0.6, 0.8$) were prepared using standard solid state methods.⁶ Dense samples (typically ≥95% theoretical) were obtained by isostatically pressing the powders into pellets at 620 MPa for 5 min, and sintering at 1650°C for 10 h. Both four-probe dc and two-probe ac measurements were used to measure the total conductivity. Ionic transference numbers of the mixed conducting oxides were determined using an electromotive force (emf) technique. Details of the sample preparation and description of the experimental setup used have been reported elsewhere.⁶

Cathodic overpotentials of mixed-conducting (Pr doped) electrodes on a Ba(Ce_{0.8}Gd_{0.2})O_{2.9} electrolyte were measured using both impedance spectroscopy and three-electrode current interruption technique (CIT).¹⁰ The impedance measurements were performed using a Hewlett Packard 4192A LF impedance analyzer (5 Hz to 13 MHz). A standard three-electrode configuration was used for the CIT;¹¹ current was applied using a Solartron 1286 electrochemical interface, and interrupted using a fast (<1 ms) switch. A Tektronix TDS 320 oscilloscope was used to measure the voltage decay. The Ba(Ce_{0.8}Gd_{0.2})O_{2.9} electrolyte disk was polished with 320 grit SiC paper to 1-2 mm thickness, and the electrode powders were ground with ethylene glycol to form a slurry. The slurry was brush painted on to the electrolyte surface and heated between 1000 and 1550°C for 0.5-10 h to form a 20-100 μm thick porous electrode layer. The painted areas of the electrodes used in this study were 0.25 to 0.45 cm². Platinum gauze applied with platinum paste was used as the current collector, and counter (anode) and reference electrodes. The measurements were performed under fuel cell conditions with dry air as the oxidant and H₂/3% H₂O as the fuel. The sintering schedule was varied for each electrode to study the effect of the morphology [examined using scanning electron microscopy (SEM)] on the cathodic overpotential resistance.

Results and Discussion

Structure.—The X-ray diffraction (XRD) patterns of all the samples could be indexed using an orthorhombic perovskite cell.¹² The decreasing lattice volume of the perovskite unit cell with increasing Pr content (Fig. 1) indicates that Pr is primarily present in the 4+ state ($r_{Ce^{4+}} = 0.87$ Å, $r_{Pr^{4+}} = 0.85$ Å, and $r_{Pr^{3+}} = 0.99$ Å). The predominance of the tetravalent state for Pr in Ba-based perovskites has also been confirmed by electron paramagnetic resonance (EPR) measurements on BaPrO₃.¹³ However, thermogravimetric analysis (TGA) indicated that the Pr-doped samples were more easily

* Electrochemical Society Active Member.

** Electrochemical Society Fellow.

^a Present address: Los Alamos National Laboratory, Los Alamos, New Mexico 87545.

^z E-mail: mukundan@lanl.gov

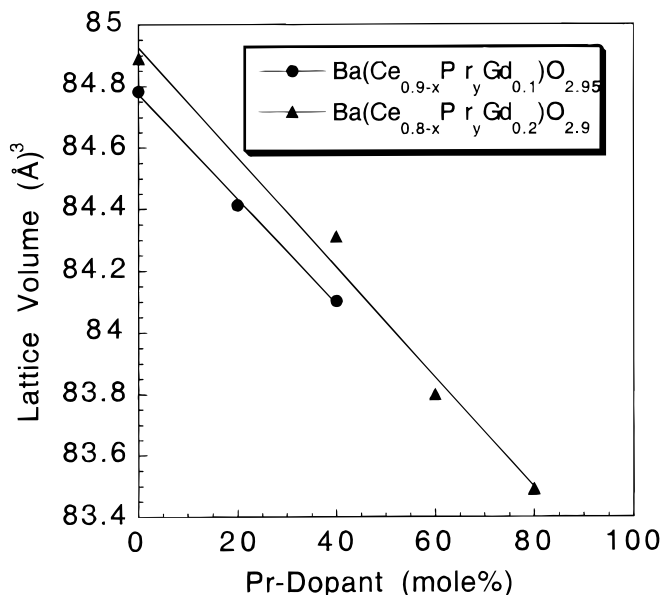


Figure 1. Lattice volumes of the perovskite unit cells for compositions in the $\text{Ba}(\text{Ce}_{0.8-y}\text{Pr}_y\text{Gd}_{0.2})\text{O}_{2.9}$ and $\text{Ba}(\text{Ce}_{0.9-y}\text{Pr}_y\text{Gd}_{0.1})\text{O}_{2.95}$ systems.

reduced than the undoped cerate. For example, while there is no significant reduction of $\text{Ba}(\text{Ce}_{0.9}\text{Gd}_{0.2})\text{O}_{2.9}$ in 5% $\text{H}_2/3\% \text{H}_2\text{O}/\text{argon}$ ($p_{\text{O}_2} = 10^{-18}$ Pa) at 700°C, under these conditions, ~70% of the Pr cations in $\text{Ba}(\text{Ce}_{0.8-y}\text{Pr}_y\text{Gd}_{0.2})\text{O}_{2.9}$ can be reduced to the 3+ state. The as-prepared Pr samples were black and changed to a brown color upon reduction, which could indicate p-type electronic conductivity. The electrical properties of the Pr solid solutions have been measured to confirm this inference, and the results for the electronic, oxygen-ionic, and protonic contributions to the conductivity are described below.

Conductivity.—The total conductivity of $\text{Ba}(\text{Ce}_{0.8-y}\text{Pr}_y\text{Gd}_{0.2})\text{O}_{2.9}$ with $y = 0.4, 0.6,$ and 0.8 (measured in dry oxygen, $p_{\text{O}_2} = 1$ atm) is shown in Fig. 2. The ionic conductivity of undoped $\text{Ba}(\text{Ce}_{0.8}\text{Gd}_{0.2})\text{O}_{2.9}$ under oxygen-hydrogen fuel cell conditions² is also shown for comparison. The total conductivity in oxygen is predominantly electronic and increases with increasing Pr content. The increase in the total conductivity induced by the substitution of Pr is consistent with the results obtained for the 10 mol % Gd system, $\text{Ba}(\text{Ce}_{0.9-y}\text{Pr}_y\text{Gd}_{0.1})\text{O}_{2.95}$.⁶ The total conductivity of the fully substituted $\text{Ba}(\text{Pr}_{0.8}\text{Gd}_{0.2})\text{O}_{2.9}$ end-member is 0.75 S/cm in air at 800°C, which is more than one order of magnitude higher than that of $\text{Ba}(\text{Ce}_{0.8}\text{Gd}_{0.2})\text{O}_{2.9}$ in wet air (5×10^{-2} S/cm)² at the same temperature.

The total conductivities of the $\text{Ba}(\text{Ce}_{0.8-y}\text{Pr}_y\text{Gd}_{0.2})\text{O}_{2.9}$ solid solutions are similar to those determined for the $\text{Ba}(\text{Ce}_{0.9-y}\text{Pr}_y\text{Gd}_{0.1})\text{O}_{2.95}$ solid solutions; see, for example, the data for $\text{Ba}(\text{Ce}_{0.5}\text{Pr}_{0.4}\text{Gd}_{0.1})\text{O}_{2.95}$ and $\text{Ba}(\text{Ce}_{0.4}\text{Pr}_{0.4}\text{Gd}_{0.2})\text{O}_{2.9}$ in Fig. 3. However, emf cell measurements indicate that a higher concentration of Gd content enhances the ionic (oxygen-ion and proton) conductivity. For example, the proton conductivity has been estimated using the proton transference number, obtained in a wet argon/dry argon cell measurement, and then multiplying it by the total conductivity in argon. For $\text{Ba}(\text{Pr}_{0.8}\text{Gd}_{0.2})\text{O}_{2.9}$ the proton conductivity is $\sim 3 \times 10^{-2}$ S/cm at 800°C, compared to 6×10^{-3} S/cm determined for $\text{Ba}(\text{Ce}_{0.5}\text{Pr}_{0.4}\text{Gd}_{0.1})\text{O}_{2.95}$.

The oxygen-ion conductivity has been obtained from the emf of a dry oxygen/dry argon cell, and from the average conductivity of the samples in oxygen and argon. At 800°C, the oxygen ion conductivities are $\approx 2 \times 10^{-2}$ S/cm and 3×10^{-3} S/cm for $\text{Ba}(\text{Pr}_{0.8}\text{Gd}_{0.2})\text{O}_{2.9}$ and $\text{Ba}(\text{Ce}_{0.5}\text{Pr}_{0.4}\text{Gd}_{0.1})\text{O}_{2.95}$, respectively. Although the ionic conductivities of the 20 mol % Gd Pr-doped sam-

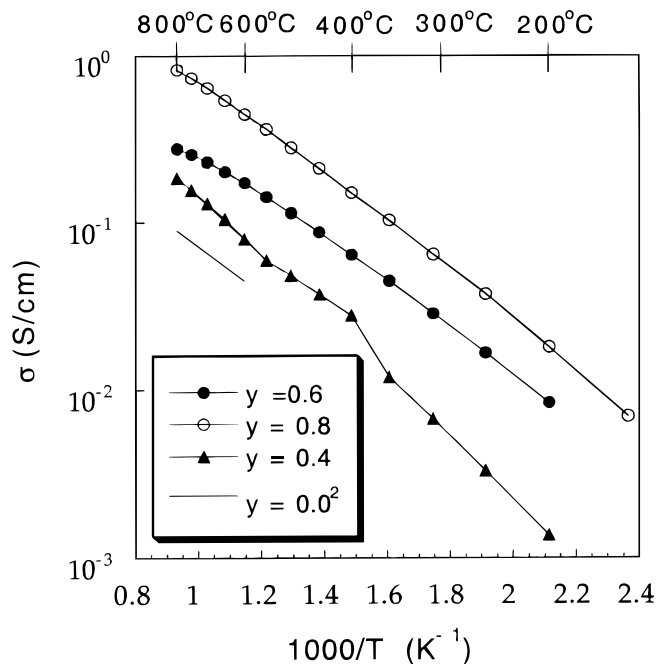


Figure 2. Total conductivity of $\text{Ba}(\text{Ce}_{0.8-y}\text{Pr}_y\text{Gd}_{0.2})\text{O}_{2.9}$, with $y = 0.4, 0.6,$ and 0.8 under dry oxygen. The ionic conductivity of $\text{Ba}(\text{Ce}_{0.8}\text{Gd}_{0.2})\text{O}_{2.9}$ under $\text{O}_2\text{-H}_2$ fuel cell conditions is shown for comparison.²

ples are higher than the 10 mol % Gd Pr-doped system, they are still somewhat lower than the values reported for the undoped $\text{Ba}(\text{Ce}_{0.8}\text{Gd}_{0.2})\text{O}_{2.9}$ end-member (0.1 S/cm at 800°C)².

Cathodic overpotentials.—Cathodic overpotentials of the Pr-doped mixed-conducting oxides and platinum electrodes in a $\text{Ba}(\text{Ce}_{0.8}\text{Gd}_{0.2})\text{O}_{2.9}$ electrolyte cell have been measured by both CIT and ac impedance. The impedance plot of a $\text{Pt}(\text{O}_2) // \text{Ba}(\text{Ce}_{0.8}\text{Gd}_{0.2})\text{O}_{2.9} // \text{Pt}(\text{wet H}_2)$ cell at $T = 800^\circ\text{C}$ is illustrated in

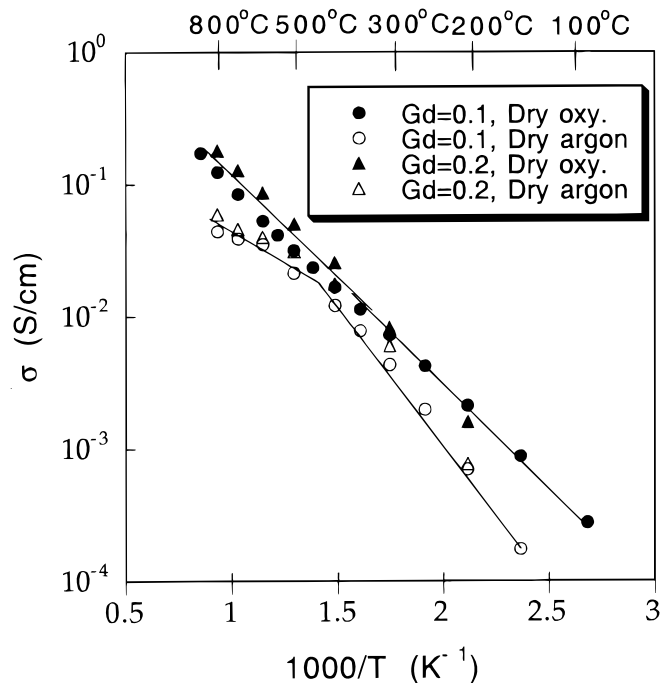


Figure 3. Comparison of the total conductivity in oxygen and argon of $\text{Ba}(\text{Ce}_{0.5}\text{Pr}_{0.4}\text{Gd}_{0.1})\text{O}_{2.95}$ and $\text{Ba}(\text{Ce}_{0.4}\text{Pr}_{0.4}\text{Gd}_{0.2})\text{O}_{2.9}$.

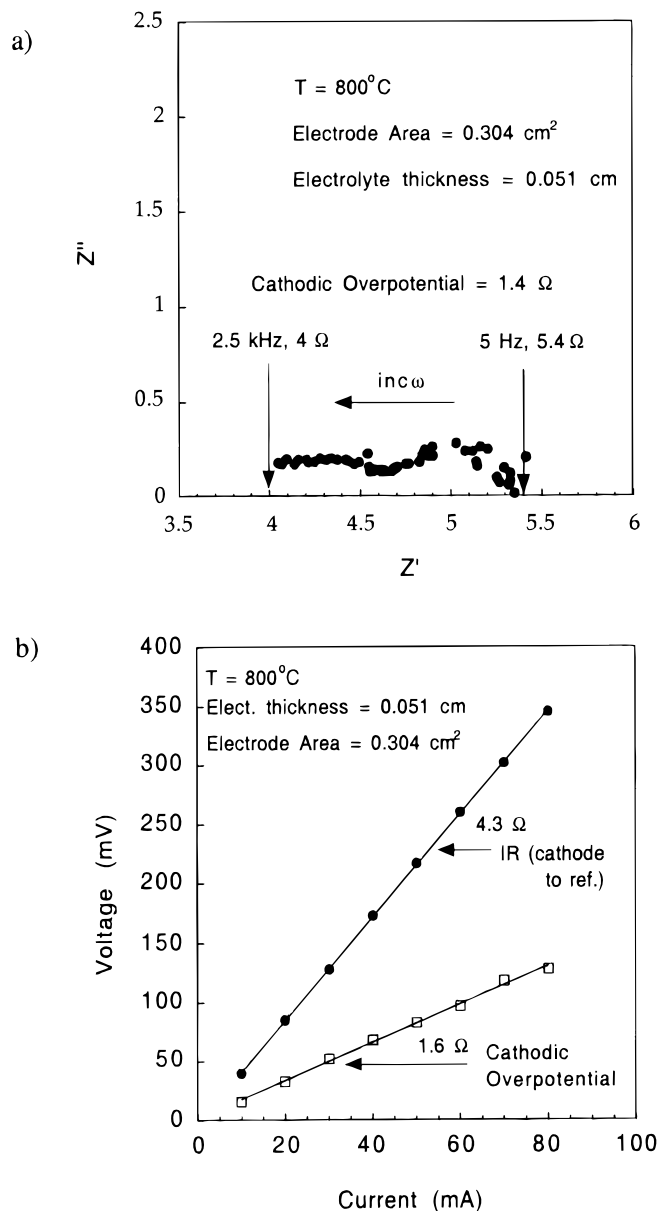


Figure 4. Comparison of the IR drop (from cathode to reference electrode) and cathodic overpotential resistance of the Pt cathode measured by ac impedance and CIT, respectively. The cell configuration is Pt(O₂) // Ba(Ce_{0.8}Gd_{0.2})O_{2.9} // Pt(wet H₂).

Fig. 4a. The left intercept on the x-axis of the impedance data plot corresponds to the partial (cathode to the reference electrode) electrolyte resistance (4 Ω), while the right intercept (5.4 Ω) represents

Table I. Comparison of the cathodic overpotential resistance measured using current interruption and the ac impedance techniques. The cell is cathode (air) // Ba(Ce_{0.8}Gd_{0.2})O_{2.9} // Pt (wet H₂). T = 800°C.

Cathode composition	$\eta_{\text{Cathode}} (\Omega)$ (CIT)	$\eta_{\text{Cathode}} (\Omega)$ (ac Impedance)	Electrode area (cm ²)
Platinum	2.47	2.04	0.304
Ba(Ce _{0.7} Pr _{0.2} Gd _{0.1})O _{2.95}	7.51	5.05	0.317
Ba(Ce _{0.5} Pr _{0.4} Gd _{0.1})O _{2.95}	4.18		0.34
Ba(Ce _{0.4} Pr _{0.4} Gd _{0.2})O _{2.90}	2.83	2.71	0.343
Ba(Pr _{0.8} Gd _{0.2})O _{2.90}	1.37	1.0	0.343

the sum of the electrolyte and cathodic overpotential resistances. The cathodic overpotential resistance plot has two arcs, probably corresponding to two different processes taking place at the cathode. These processes could be associated with proton transfer from the electrolyte to air, or with oxygen transfer from air to the electrolyte.

Because the measured resistances are ohmic, the cathodic overpotential resistance measured by this technique (1.4 Ω) in 1 atm O₂ at 800°C is very close to that obtained (1.6 Ω) from the CIT (Fig. 4b). In Table I, the cathodic overpotential resistance (η) in air at 800°C obtained using the CIT are compared to those obtained from the ac impedance. The resistances obtained by the ac technique are for zero current flowing through the cell while those obtained by the CIT are for a finite current (0 < i < 100 mA/cm²). The comparison in Table I shows that the values measured by the impedance technique are lower than those obtained by the CIT, indicating that the cathodic overpotential resistance shows deviations from ohmic behavior at high current densities.

The variation of the electrode overpotential with composition has been measured by the CIT using the Pr mixed-conducting cathodes prepared in identical ways in order to minimize electrode-morphology effects. The overpotentials of the Pr-doped cathodes measured in air are compared in Fig. 5. All the perovskite cathodes have been prepared by brush painting the perovskite powders on the electrolyte surface (area ~0.3 cm², thickness ~40 μm), and then sintering at 1500°C for 3 h. Figure 5 shows that the cathodic overpotential resistance decreases with increasing Pr and Gd content. The Ba(Pr_{0.8}Gd_{0.2})O_{2.9} composition has the lowest overpotential (cathodic overpotential resistance = 0.47 Ω cm² at 800°C). The decrease in the overpotential can be directly attributed to the increases in the electronic and ionic conductivity arising from the Pr and Gd substitutions, respectively. As shown in Fig. 6, the overpotential for Ba(Pr_{0.8}Gd_{0.2})O_{2.9} is the lowest cathodic overpotential resistance reported for any perovskite electrode on a proton-conducting electrolyte fuel cell at 800°C. Moreover, at current densities <50 mA/cm², the polarization of the Ba(Pr_{0.8}Gd_{0.2})O_{2.9} cathode is comparable to that of an optimized platinum electrode.

The effect of electrode morphology on the cathodic overpotential resistances has also been investigated by using a specific cathode composition, Ba(Ce_{0.4}Pr_{0.4}Gd_{0.2})O_{2.9}, prepared by three different processing methods. One sample (A) was prepared from ballmilled powders (~1 μm particle size) and sintered at 1500°C for 3 h. Two other samples were prepared using ~5 μm powders; one (B) was sintered at 1500°C for 3 h using a glycerin binder, the other (C) was sintered at 1500°C for 10 h. The thickness of the cathodes was kept

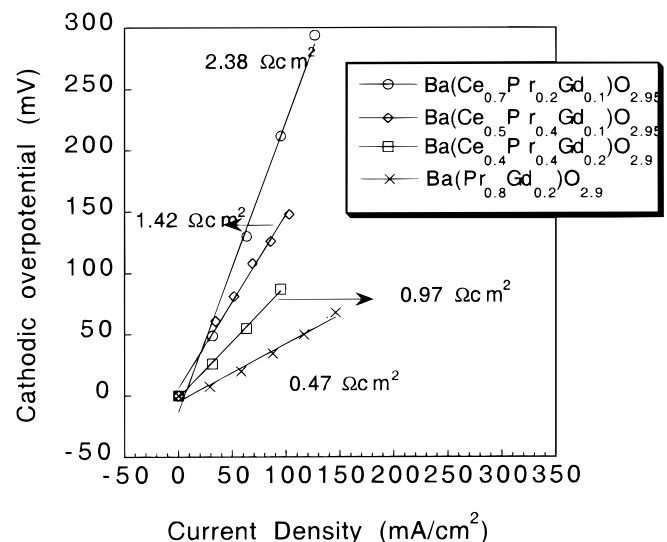


Figure 5. Comparison of the cathodic overpotential resistances of several Pr-doped barium cerate cathodes. The cell configuration is cathode (air) // Ba(Ce_{0.8}Gd_{0.2})O_{2.9} // Pt (wet H₂). T is 800°C.

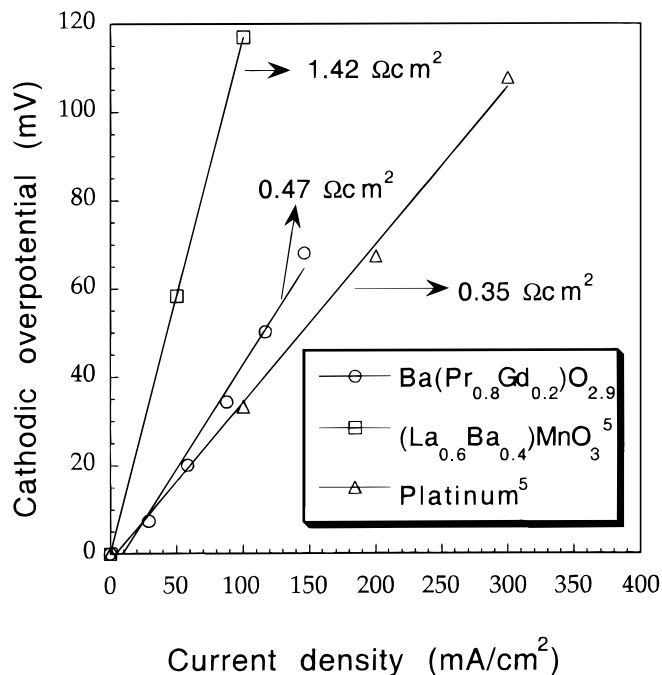


Figure 6. Comparison of the cathodic overpotential resistance (in air) of $\text{Ba}(\text{Pr}_{0.8}\text{Gd}_{0.2})\text{O}_{2.9}$ with those available in the literature. $T = 800^\circ\text{C}$.

constant by controlling the consistency of the electrode slurry and the number of layers of brush painting.

Scanning electron micrographs of the electrode surfaces are shown in Fig. 7-9. The thickness of each cathode is $\sim 40\ \mu\text{m}$, and the particle sizes range from $\sim 1\ \mu\text{m}$ (sample A) to $\sim 5\ \mu\text{m}$ (samples B and C). Although the relationship between the electrode morphology and its overpotential has not been quantitatively examined, morphology effects appear to be less significant than the effects due to changes in the cathode composition. For example, Fig. 10 shows that the cathodic overpotential resistances of the three samples of the $\text{Ba}(\text{Ce}_{0.4}\text{Pr}_{0.4}\text{Gd}_{0.2})\text{O}_{2.9}$ electrodes varied from 0.68 to $1.26\ \Omega\ \text{cm}^2$, with all three values being higher than that observed for $\text{Ba}(\text{Pr}_{0.8}\text{Gd}_{0.2})\text{O}_{2.9}$ ($0.47\ \Omega\ \text{cm}^2$) and lower than those for $\text{Ba}(\text{Ce}_{0.5}\text{Pr}_{0.4}\text{Gd}_{0.1})\text{O}_{2.95}$ ($1.42\ \Omega\ \text{cm}^2$). These results indicate that the compositional trends in the overpotentials are valid irrespective of morphological considerations. However, for a given composition,

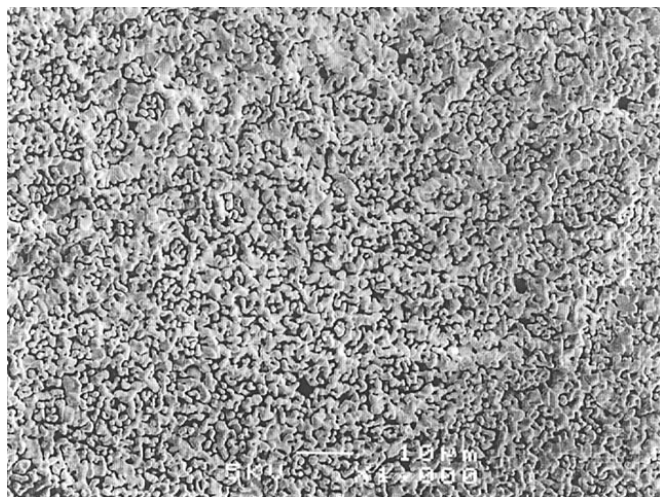


Figure 7. SEM of a $\text{Ba}(\text{Ce}_{0.4}\text{Pr}_{0.4}\text{Gd}_{0.2})\text{O}_{2.9}$ electrode (sample A). The slurry was prepared from ballmilled powders mixed in ethylene glycol. The electrode was sintered at 1500°C for 3 h.

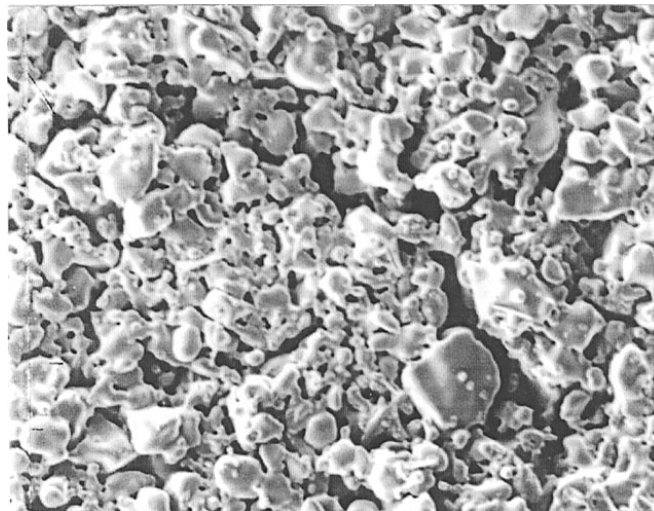


Figure 8. SEM of a $\text{Ba}(\text{Ce}_{0.4}\text{Pr}_{0.4}\text{Gd}_{0.2})\text{O}_{2.9}$ electrode (sample B). The slurry was prepared using glycerin binder, and the electrode was sintered at 1500°C for 3 h.

the magnitude of the overpotential could be minimized by tailoring the cathode morphology.

Conclusions

p-Type electronic conductivity is introduced into $\text{Ba}(\text{Ce}_{1-x}\text{Gd}_x)\text{O}_{3-x/2}$ by the substitution of Pr for Ce. Higher concentrations of Pr ($\geq 40\ \text{mol}\%$) induce significant increases in the total conductivity due to the enhancement of the p-type electronic conductivity. Fully substituted samples of $\text{Ba}(\text{Pr}_{0.8}\text{Gd}_{0.2})\text{O}_{2.9}$ have the highest total conductivity with $\sigma_T = 0.75\ \text{S/cm}$ in air at 800°C . The measured overpotentials of the Pr-doped cathodes decrease with increasing ionic and electronic conductivity. The overpotential ($0.47\ \Omega\ \text{cm}^2$) obtained for the $\text{Ba}(\text{Pr}_{0.8}\text{Gd}_{0.2})\text{O}_{2.9}$ cathode is the lowest reported for a perovskite electrode in a proton-conducting electrolyte fuel cell at 800°C .

Acknowledgments

The financial support of the Electric Power and Gas Research Institutes (EPRI and GRI) and the New Energy and Industrial Technology Development Organization (NEDO) is gratefully acknowl-

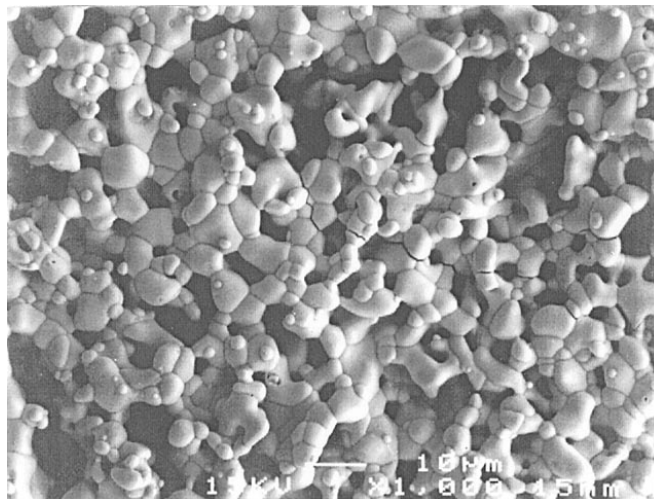


Figure 9. SEM of a $\text{Ba}(\text{Ce}_{0.4}\text{Pr}_{0.4}\text{Gd}_{0.2})\text{O}_{2.9}$ electrode (sample C). The slurry was prepared using ethylene-glycol, and the electrode was sintered at 1500°C for 10 h.

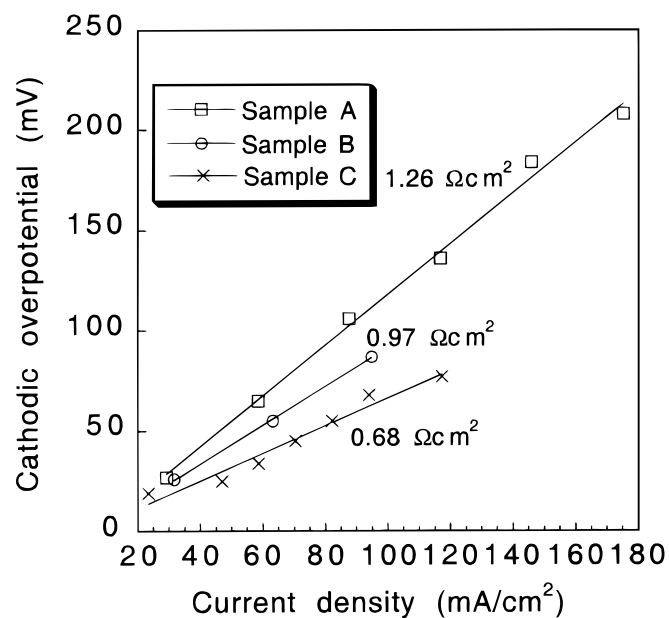


Figure 10. Comparison of the cathodic overpotential resistance of $\text{Ba}(\text{Ce}_{0.4}\text{Pr}_{0.4}\text{Gd}_{0.2})\text{O}_{2.9}$, prepared by three different methods (see text for details). The cell is cathode (air) // $\text{Ba}(\text{Ce}_{0.8}\text{Gd}_{0.2})\text{O}_{2.9}$ // Pt (wet H_2), $T \approx 800^\circ\text{C}$.

edged. This research was conducted in the Laboratory for Research on the Structure of Matter (LRSM) at the University of Pennsylvania that is supported by the National Science Foundation. The authors also thank W. Romanov and R. Chao for their help in sample preparation, and H. Ping for useful discussions and help in assembling the equipment.

Los Alamos National Laboratory assisted in meeting the publication costs of this article.

References

1. H. Iwahara, T. Esaka, H. Uchida, and N. Maeda, *Solid State Ionics*, **3/4**, 359 (1981).
2. N. Taniguchi, K. Hatoh, J. Niikura, T. Gamo, and H. Iwahara, *Solid State Ionics*, **53-56**, 998 (1992).
3. N. Bonanos, B. Ellis, K. S. Knight, and M. N. Mahmood, *Solid State Ionics*, **35**, 179 (1989).
4. N. Bonanos, B. Ellis, and M. N. Mahmood, *Solid State Ionics*, **44**, 305 (1991).
5. H. Iwahara, T. Yajima, H. Uchida, and K. Morimoto, in *Proceedings of 2nd International Symposium on Solid Oxide Fuel Cells*, p. 229, Athens, Greece (1991).
6. R. Mukundan, P. K. Davies, and W. L. Worrell, *Ceram. Trans.*, **65**, 13 (1996).
7. R. Mukundan, P. K. Davies, and W. L. Worrell, *Mater. Res. Soc. Symp. Proc.*, **453**, 573 (1997).
8. T. Fukui, S. Ohara, and S. Kawatsu, *J. Power Sources*, **71**, 164 (1998).
9. T. Fukui, S. Ohara, and S. Kawatsu, *Solid State Ionics*, **116**, 331 (1999).
10. D. Y. Wang, and A. S. Nowick, *J. Electrochem. Soc.*, **126**, 1155 (1979).
11. M. Nagata, Y. Itoh, and H. Iwahara, *Solid State Ionics*, **67**, 215 (1994).
12. A. J. Jacobson, B. C. Tofield, and B. E. F. Fender, *Acta Crystallogr.*, **B28**, 956 (1972).
13. Y. Hinatsu, *J. Solid State Chem.*, **102**, 362 (1993).